ABSTRACT

Report on the impact on the stability and accuracy of aerosol retrieval (day vs. night) of using the LIME vs. the RIMO correction factor (RCF) lunar irradiance model as reference, which accounts for a correction factor to provide accurate lunar photometric aerosol measurements, and also the impact on the ROLO/RIMO model.

Africa Barreto, Carlos Toledano, Ramiro González, Javier Gatón, David Mateos

University of Valladolid, AEMET

20 April 2023

D-5: Report on the impact of using the LIME model on the stability and accuracy of aerosol retrieval (day vs. night)

[Document subtitle]

This document was produced as part of the ESA-funded project “Improving the Lunar Irradiance Model of ESA” under ESA contract number: ESA-EOPG-EOPGMQ-SOW-24

Signatures and version history

	Name	Organisation	Date
Written by			
Written by			
Written by			
Reviewed by (consortium)			
Approved by (ESA)			

Version history

Version	Date	Publicly available or private to consortium?

Contents

1 Introduction

1.1 Purpose and Scope

This document forms deliverable D-5 of the ESA project: "Improving the Lunar Irradiance Model of ESA". Its purpose is to report the impact on the stability and accuracy of aerosol retrieval (day vs. night) of using the LIME (version v01) vs. the RIMO correction factor (RCF) lunar irradiance model as reference, which accounts for a correction factor to provide accurate lunar photometric aerosol measurements, comparing also the impact on AOD using the ROLO/RIMO model.

1.2 Applicable and reference documents

Number	Reference
[AD1]	Roberto Román , Ramiro González , Carlos Toledano , África Barreto , Daniel Pérez-Ramírez, Jose A. Benavent-Oltra , Francisco J. Olmo , Victoria E. Cachorro , Lucas Alados-Arboledas and Ángel M. de Frutos, Correction of a lunar irradiance model for aerosol optical depth retrieval and comparison with star photometer, Preprint. Atmospheric Measurement Techniques, Discussion started: 10 August 2020, https://doi.org/10.5194/amt-2020-293
[AD2]	Ramiro González, Carlos Toledano, Roberto Román, David Fuertes, Alberto Berjón, David Mateos, Carmen Guirado-Fuentes, Cristian Velasco-Merino, Juan Carlos Antuña-Sánchez, Abel Calle, Victoria E. Cachorro, and Ángel M. de Frutos, Daytime and nighttime aerosol optical depth implementation in CÆLIS. Geosci. Instrum. Method. Data Syst., 9, 417–433, https://doi.org/10.5194/gi-9-417-2020, 2020.
[AD3]	África Barreto, Emilio Cuevas, Bahaidin Damiri, Carmen Guirado, Timothy Berkoff, Alberto Jesús Berjón, Yballa Hernández, Fernando Almansa, and Manuel Gil, M.: A new method for nocturnal aerosol measurements with a lunar photometer prototype, Atmos. Meas. Tech., 6, 585–598, doi:10.5194/amt-6-585-2013, 2013.
[AD4]	África Barreto, Emilio Cuevas, María José Granados-Muñoz, Lucas Alados-Arboledas, Pedro Miguel Romero, Julian Gröbner, Natalia Kouremeti, Fernando Almansa, Thomas Stone, Carlos Toledano, Roberto Román, Mikhail Sorokin, Brent Holben, Marius Canini and Margarita Yela: The new sun-sky-lunar Cimel CE318-T multiband photometer – a comprehensive performance evaluation, Atmos. Meas. Tech., 9, 631–654, https://doi.org/10.5194/amt-9-631-2016, 2016.

1.3 Glossary

1.3.1 Abbreviations

Abbreviation	Stands For	Notes
Cimel	(Not an abbreviation)	Instrument manufacturer, also used as shorthand for instrument itself. Model CE318, CE318-TS or CE318-TP

AOD	Aerosol Optical Depth	Measure of atmospheric aerosols in the atmospheric column
ROLO	Robotic Lunar Observatory	Lunar exo-atmospheric irradiance model developed by USGS
RIMO	ROLO implementation for Moon photometry observation	Lunar exo-atmospheric irradiance model developed by AEMET, University of Valladolid, University of Granada, ISAC and the Czech Academy of Sciences
RCF	RIMO Correction Factor	Lunar exo-atmospheric irradiance model developed by University of Valladolid and AEMET as a correction of the RIMO model
CÆLIS	Not an abbreviation	Software tool to process photometric information developed at University of Valladolid

2 Importance of AOD monitoring at night

Back to the 90's, sunlight photometric measurements were, with other remote sensing techniques, the most common method to study atmospheric aerosols, providing reliable information about optical, micro-physical and radiative aerosol properties of these important atmospheric constituents. With this valuable information long-term and global Aerosol Optical Depth (AOD) records and other aerosol properties were compiled in order to better understand the role of aerosols in the Earth's climate. The principal drawback of sun photometry is that they provide information limited to daytime, making full diurnal (24h) aerosol monitoring and characterization impossible. This is a severe constrain when it comes to study atmospheric processes in which day-to-night variations play an important role, introducing a bias in climatological studies which is critical for high latitude and polar regions.

One of the most important pioneering attempts to estimate AOD at night developed were developed by Herber et al. (2002). These authors provided, for the first time, a long-term (9-year) database of photometric measurements in the Arctic, providing us with the capability of studying the seasonal variation and trends of tropospheric aerosol using solar, lunar and stellar photometry. Berkoff et al. (2011) presented for the first time the capability of a commercial (adapted) Cimel to perform lunar measurements. However, the need to monitor aerosols in a routine way in the absence of solar radiation has led to remarkable efforts in the scientific community, especially by polar atmospheric researchers. It was the case of the development of the new Cimel CE318-U and CE318-TS versions published in Barreto et al. (2013, 2016). With this information, the CE318-TS, capable of performing solar, lunar and sky measurements, was considered in 2016 the reference instrument in the NASA-

AERONET network (Holben et al., 1998; Giles et al., 2019), the most extensive aerosol monitoring network worldwide, extending its monitoring capability to nighttime.

3 Current status of the AOD monitoring at night

There are currently only a few techniques capable of measuring AOD at night-time: lidar, stellar photometry and lunar photometry. The complexities associated to lidar and stellar photometry in terms of methodology, infrastructure and automation represent an important limitation for their operational use in global networks. Lunar photometry, despite being a simple and reliable technique with the capability of global operation, is affected by important drawbacks. First, the Moon cycle reduces the suitable nights to those in which the Moon is sufficiently bright, and the sky is dark, typically from 1st to 3rd quarter. But the most important one is related to the variability of the reflected solar irradiance with the Moon's cycle (Barreto el at., 2016). The consequence is that a precise exo-atmospheric lunar irradiance model is mandatory to derive the AOD in lunar photometry (Berkoff et al., 2011; Barreto et al., 2013, 2016; AD1).

Following [AD1], AOD from lunar irradiance observation can be calculated following the Beer-Bouguer-Lambert law as follows:

$$\tau_a(\lambda) = \frac{\ln\left(k^M(\lambda)\right) - \ln\left(V^M(\lambda) / E_0^M(\lambda)\right) - m_g \cdot \tau_g(\lambda) - m_R \cdot \tau_R(\lambda)}{m_a} \quad \text{[Eq. 1]}$$

In this equation τ_a and k^M represent the AOD and the Moon calibration coefficient respectively, for a nominal λ-wavelength, while E_0^M and V^M are the extraterrestrial lunar irradiance and the photometer lunar signal at the same nominal wavelength, respectively. m_a, m_R and m_g are the optical airmass for aerosols, Rayleigh scattering and gaseous absorption, and τ_R and τ_g represent the optical depth of Rayleigh scattering and gaseous absorption, respectively. More details about these calculation in CÆLIS can be found in [AD2].

Different methods are presented in the literature to retrieve the calibration coefficient (k^M). The Lunar Langley calibration method (AD3, AD4) is similar to a classic Langley-plot calibration but applied to nighttime period. This method requires to be applied under pristine conditions and is affected by the illumination change during the lunar cycle. However, the so called Gain calibration method (AD1,AD4) is considered a suitable technique to calculate k^M without the use of E_0^M and taking the advantage of the Cimel photometer, capable to measure during day and nighttime with the same optical configuration (same detectors used for Sun and Moon measurements with an amplification or gain factor, G). The values of G were measured with an integrating sphere in the laboratory by [AD4] and Li et al. (2016). These authors found experimental values for G differing less than 0.3% from the nominal value of 4096; hence, G is assumed in CÆLIS as wavelength independent and with a constant value of 4096. Taking into account that the only difference between Sun and Moon measurements is this Gain factor, the Sun calibration can be transferred to Moon as follows [AD1]:

$$k^M(\lambda) = \frac{V_0^S(\lambda)}{E_0^S(\lambda)} \cdot G \quad \text{[Eq. 2]}$$

In this equation, V_0^S represents the Sun calibration coefficient (retrieved with the Langley method) and E_0^S the extraterrestrial solar irradiance, extracted from Wehrli (1986) to be consistent with the ROLO computation. The Gain calibration is simpler than Lunar Langley method because it is not dependent on the RIMO (or other lunar irradiance model) and it only requires the daytime calibration, which provides more operational character to this method [AD1].

Equation 1 also shows the needed to estimate the E_0^M term. There are different sources of information to estimate extraterrestrial lunar irradiances, i.e. the lunar models, that we will briefly discuss, as they have decisive impact on the retrieval of AOD.

3.1 Robotic Lunar Observatory (ROLO)

The United States Geological Survey (USGS) ROLO model, developed by Kieffer and Stone (2005), is considered one of the most reliable lunar radiometric references, with an estimated uncertainty ranging from 5% to 10% (Stone and Kieffer, 2004). ROLO is mainly based on empirical relationships between lunar irradiances measured at 32 channels and the different geometrical factors of the Moon-observer positions. These measurements were performed by two CCD devices mounted in two twin telescopes operating in Flagstaff (Arizona). It is considered that this model has adequate precision for sensor response temporal trending but an improvement of one order of magnitude in absolute accuracy is still needed for climate studies (Stone et al., 2020). Barreto et al. (2016) observed a phase angle dependence of this model at the high-mountain Izaña Observatory, with systematic errors in the ROLO model or instrumental problems in the CE318-T photometer as the most probable causes for such dependence. Other authors also found important variations between on-orbit lunar irradiances and the irradiances predicted by the USGS/ROLO model (Viticchié et al., 2013; Lacherade et al., 2013, 2014).

3.2 ROLO implementation for Moon photometry observation (RIMO)

RIMO model, described in detail in Barreto et al. (2019), is an open-access implementation of the ROLO model (http://testbed.aemet.es/rimoapp) developed by a team formed by members of several institutions: AEMET (Izaña Observatory), University of Valladolid (Spain), University of Granada (Spain), ISAC (Italy) and the Czech Academy of Sciences (Czech Republic). RIMO is able to provide the scientific community with an accessible irradiance model for the near real-time AOD calculations required for aerosol monitoring, using the same empirical formulation in terms of lunar-disk equivalent reflectance presented in Kieffer and Stone (2005), but taking into account a misleading description of the different variables (T. Stone, personal communication in the 3rd Lunar Workshop, Izaña, 2017).

The formulation of the RIMO model has been implemented in CÆLIS [AD2].

3.3 RIMO Correction Factor (RCF)

[AD1] used Cimel CE318-TS measurements performed in 98 pristine nights with low and stable AOD at the Izaña Observatory (Tenerife, Spain) to correct the inaccuracies previously observed in the ROLO/RIMO model. Differences between the AOD obtained using RIMO and the expected day-night-day AOD evolution under such pristine conditions were used to estimate by linear interpolation a correction factor for RIMO (RCF), dependent on the spectral band, the lunar phase angle and the lunar zenith angle. Therefore, this RCF is a proposed correction factor that, multiplied by RIMO value, gives an effective extraterrestrial lunar irradiance that provides AOD values with lower uncertainty than the RIMO itself (expected uncertainty in AOD between 0.03 and 0.01), being considered currently a reference for AOD calculation at night (AD1).

3.4 LIME

In the context of this project, the LIME model in its version v01 is considered another source of information to estimate the E_0^M term in Equation 1 for AOD monitoring at night.

4 Results

In this section we assess the impact of the improved LIME (v01) modelling capabilities in the AOD calculation at night using the RCF model as reference. Figure 1 shows boxplots with the AOD differences calculated using RCF and other models (RIMO or LIME) as lunar extraterrestrial irradiance model (E_0^M) in Eq. 1. The Gain calibration method has been used in the three AOD retrievals. Taking into account that the processing in the AOD calculation is the same for the three AOD products, the difference in the AOD observed between the three dataset is directly related to the impact of the estimation of the E_0^M term. Important outliers were detected in the case of the AOD calculated with the LIME model on May 15-16, 2022 (see Figure 2), when a total lunar eclipse occurred. This specific night was excluded from the subsequent analysis.

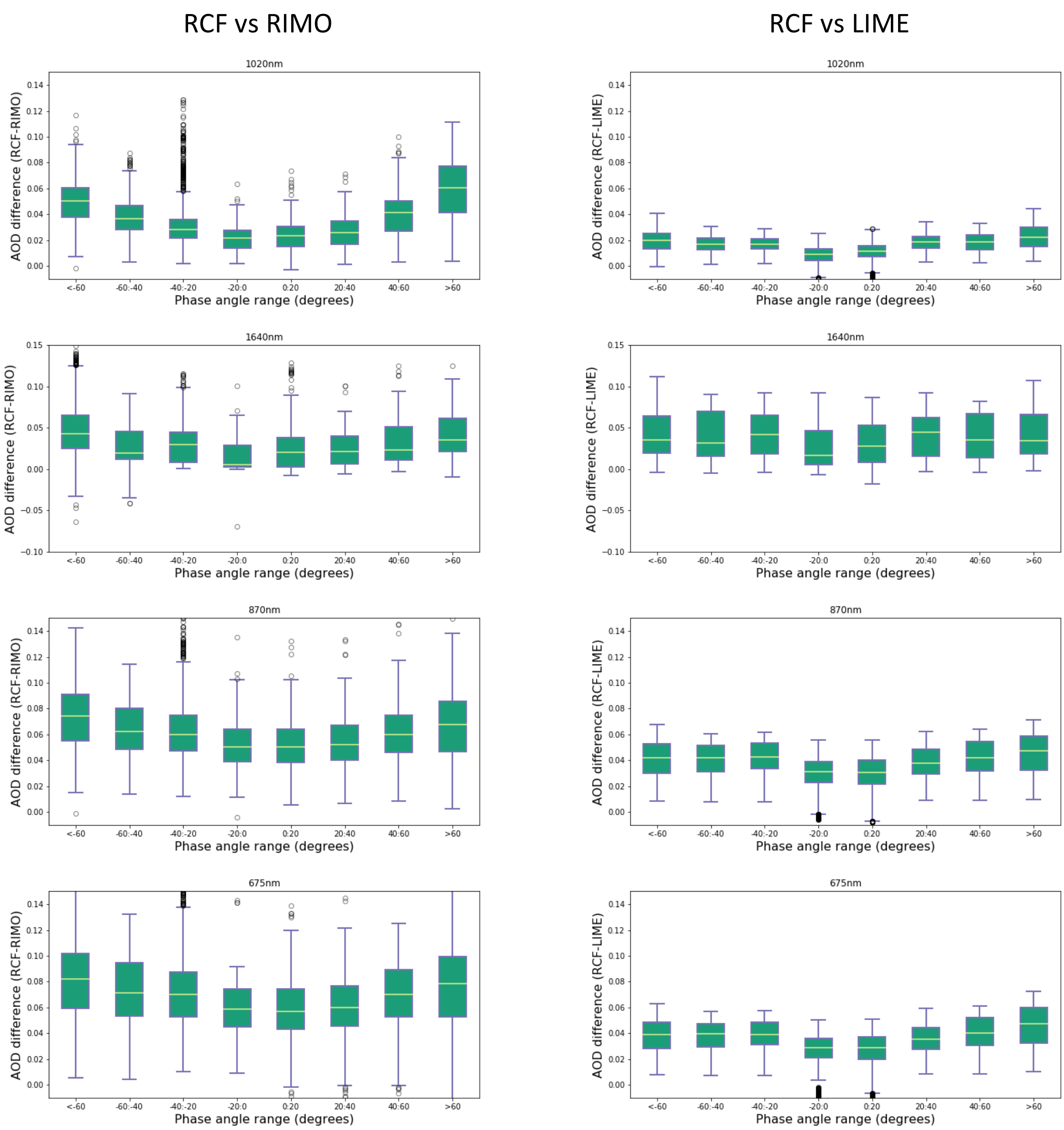

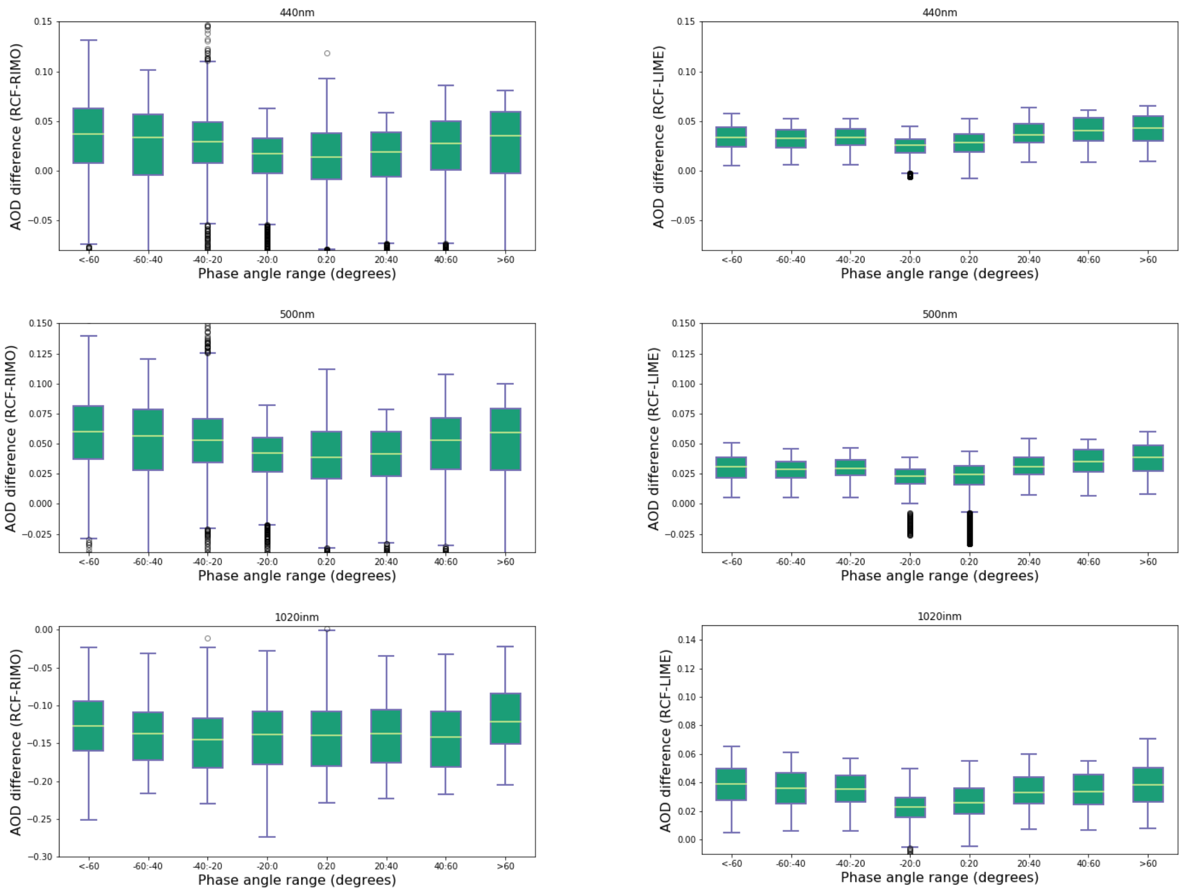

Figure 1: Boxplots with the AOD difference for the six different CE318-TS spectral bands and different ranges of lunar phase angles using the RCF in the AOD calculation as reference. The comparison with the AOD calculated with RIMO is shown in the left column and with the LIME in the right column. Lower and upper boundaries for each box are the 25 and 75 percentiles, the solid line is the median value and circles indicate values out of the 1.5 fold box area (outliers, out of the range of the axis).

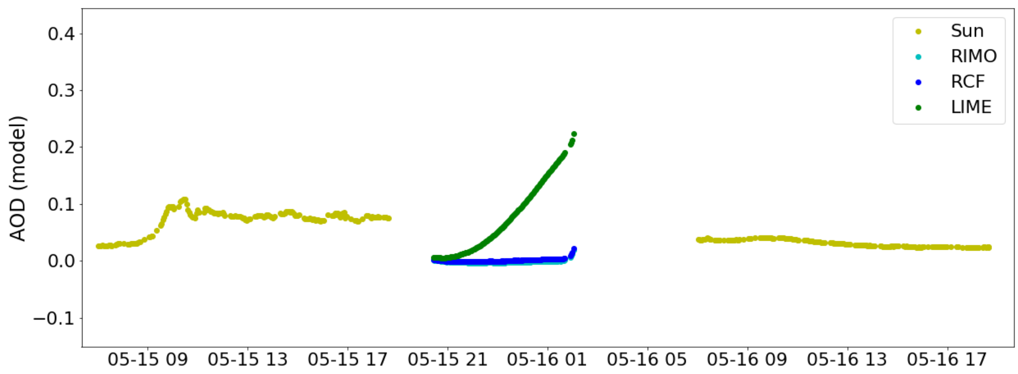

Figure 2: AOD measured at 1640 nm spectral band in Teide Peak station during a sequence of 2 days, including daytime data (yellow), and also AOD at night using the RCF, RIMO and LIME as lunar exo-atmospheric irradiance models. A total lunar eclipse occurred this night, between May 15-16, 2022.

Figure 3 presents the scatterplot between the reference AOD at night (RCF) and the AOD calculated using RIMO and LIME models, including common statistics such as number of coincident points (N), linear fitting coefficients and regression coefficient (r). Standard error of these two fitting plots and their relative differences have been included in Table 1 in order to quantify the improvement that the LIME model introduces in term of AOD. The main results that can be extracted from these complementary pieces of information can be summarized as follows:

1. There is a better performance of LIME with regard the lunar phase angle (RCF-LIME AOD differences are smaller compared to those between RCF and RIMO).
2. There is an appreciable reduction in the average AOD difference associated with the use of the LIME model in relation to the RIMO model in all channels except in the 1640 nm spectral band (see Figure A1).
3. Higher dispersion of AOD differences has been observed in the case of the RIMO model, especially in the 440 nm spectral band. Figure 4 shows an AOD evolution observed at Teide Peak station in this specific CE318-TS band. The presence of an important zenith angle dependence of the AOD at night is observed in the case of the AOD retrieved using the RIMO model.
4. The improvement of the LIME model is appreciable by looking Table 1 (from 95 to 33%), with considerably low standard errors of the fitting, below 0.02 in all cases with the exception of 1640 nm spectral band. 1020 InGaAs spectral band also presents low standard errors but considerably higher (one order of magnitude) than the same spectral band measured with the Silicon detector. As previously stated in [AD1], considerably high discrepancies were observed in the fitting coefficients of the RCF value for 1020 nm Silicon and InGaAs which could be attributed to the existence of different Gain factors in the two detector's signal.

(a)

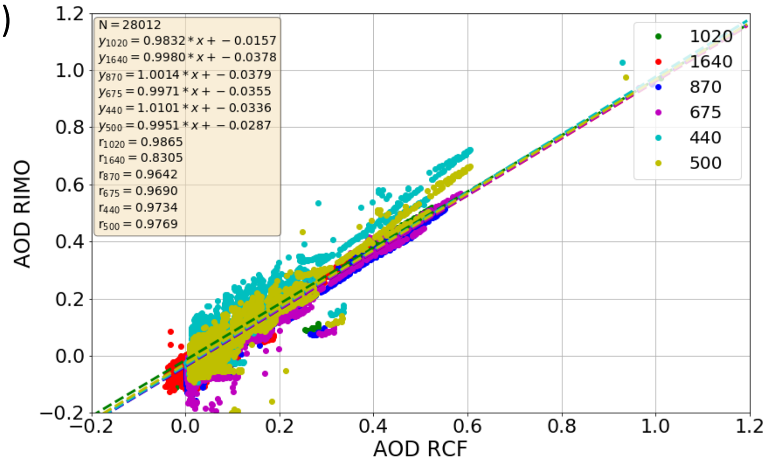

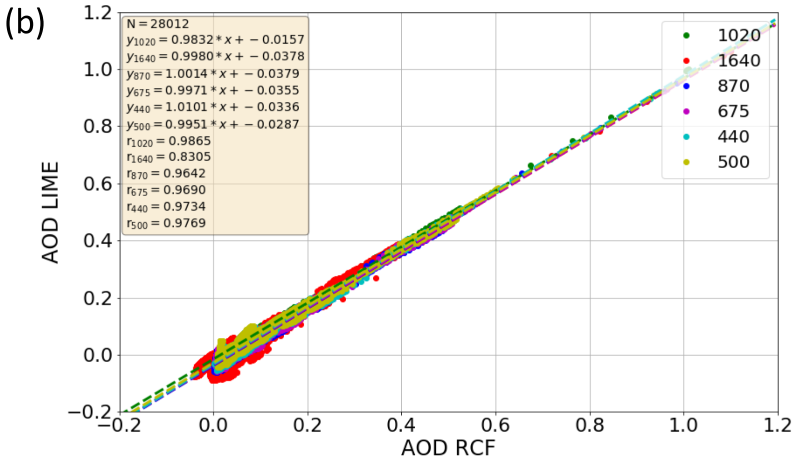

Figure 3: Scatterplot between the AOD retrieved using RCF as reference and the AOD calculated using (a) RIMO and (b) LIME, for the six different spectral bands of the CE318-TS. Statistics of the fitting plots are also included in the text box, with number of points (N), linear fitting coefficients and regression coefficient (r). Axis in (a) have been adapted to those in (b), and therefore outliers are not visible in this graph.

BAND	RCF-RIMO	RCF-LIME	REL. DIFF. (RIMO VS LIME)
1020	0.020	0.001	-95%
1640	0.023	0.027	17%
870	0.021	0.014	-33%
675	0.027	0.014	-48%
440	0.087	0.013	-85%
500	0.049	0.012	-75%
1020 I	0.046	0.016	-74%

Table 1: Standard error of the fitting plot between AOD retrieved using RCF and those AOD values retrieved using RIMO/LIME extraterrestrial lunar irradiance models, including the relative differences between the two standard errors.

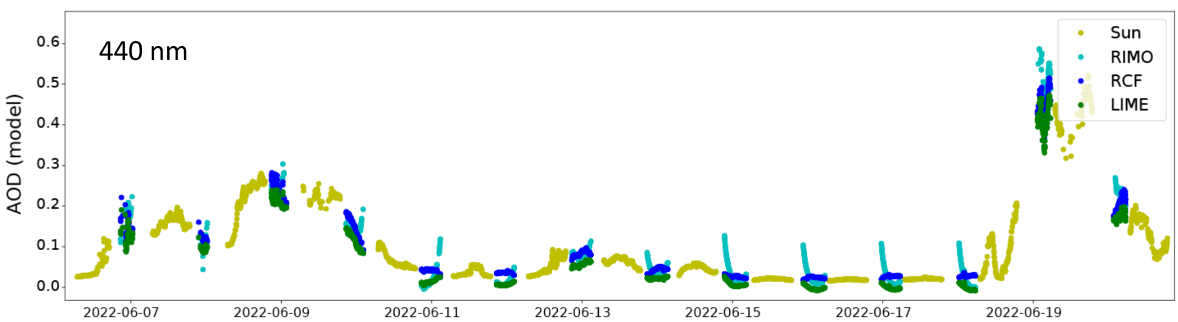

Figure 4: AOD measured at 440 nm spectral band in Teide Peak station in a sequence of 14 days (yellow) and nights in the frame of the current ESA project. Nocturnal AOD products have been retrieved using RIMO, RCF and LIME as lunar extraterrestrial irradiance models.

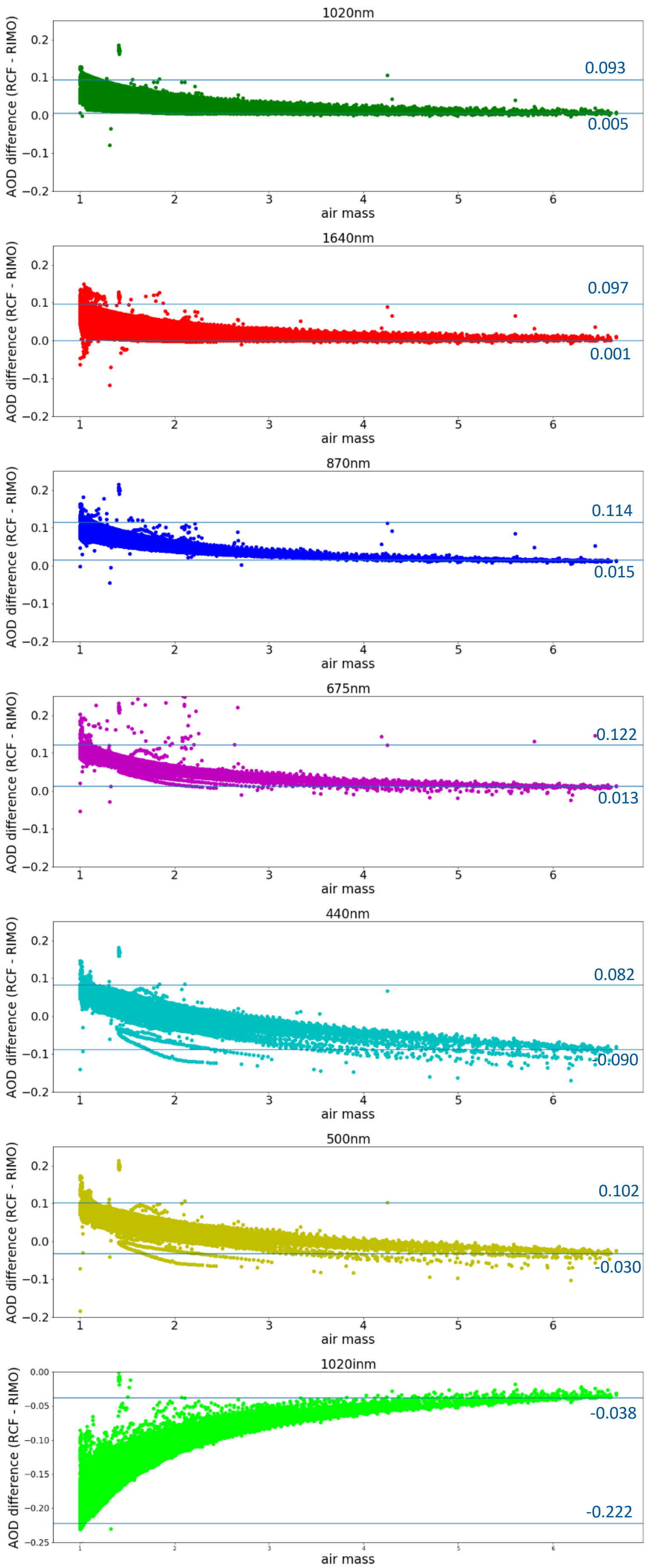
1020nm
AOD difference (RCF - RIMO)
air mass
0.093
0.005
1640nm
AOD difference (RCF - RIMO)
air mass
0.097
0.001
870nm
AOD difference (RCF - RIMO)
air mass
0.114
0.015
675nm
AOD difference (RCF - RIMO)
air mass
0.122
0.013
440nm
AOD difference (RCF - RIMO)
air mass
0.082
-0.090
500nm
AOD difference (RCF - RIMO)
air mass
0.102
-0.030
1020inm
AOD difference (RCF - RIMO)
air mass
-0.038
-0.222

Figure 5: AOD difference (RCF versus RIMO) with air mass for the different Cimel spectral bands. Percentiles 99 and 1 are included as horizontal lines. Y-scale has been reduced to cover the -0.2-0.25 AOD range.

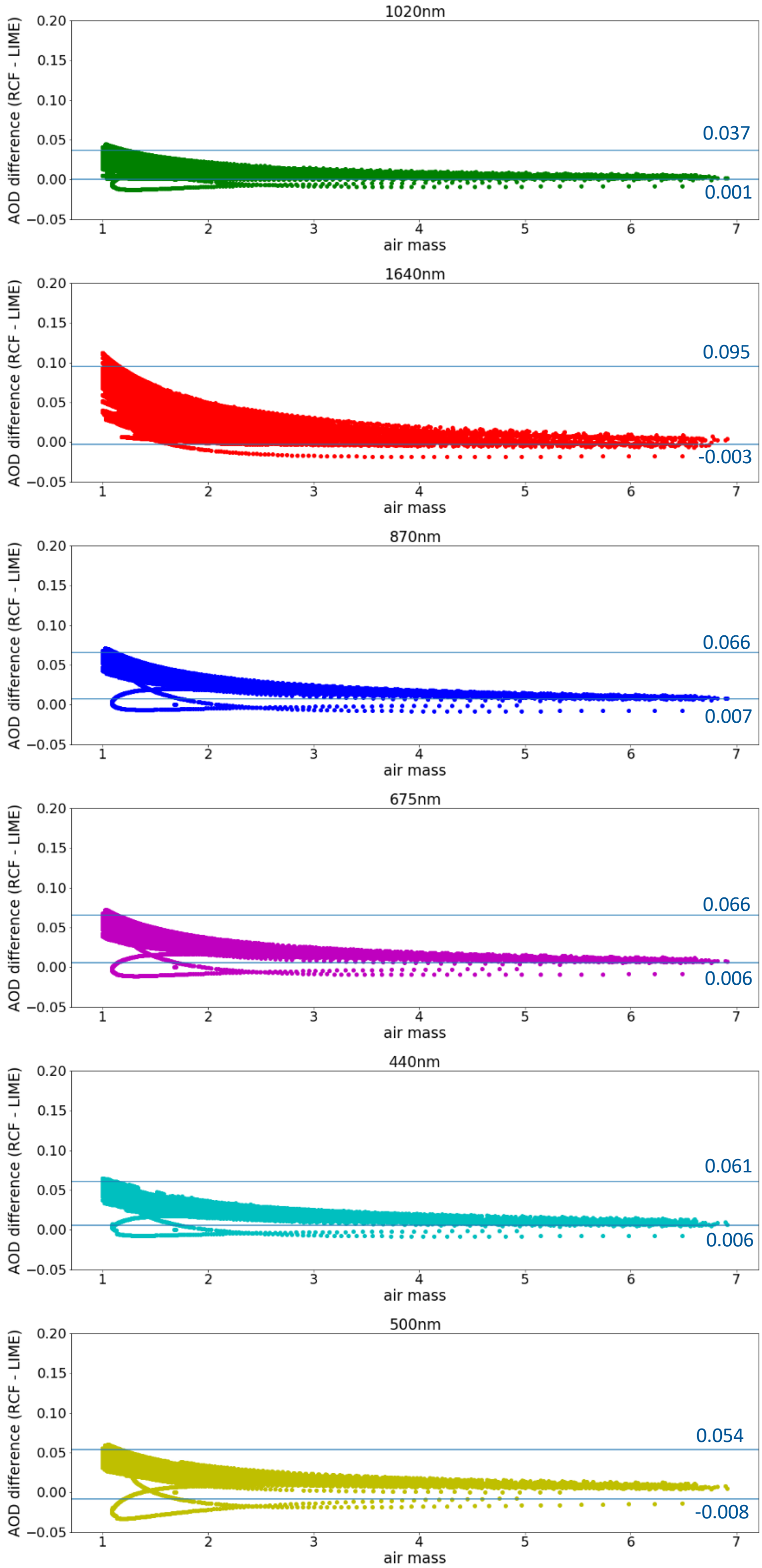

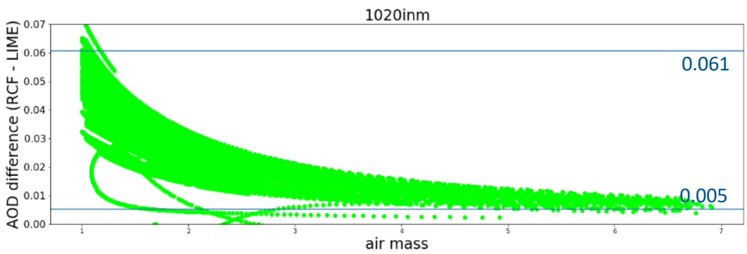

Figure 6: AOD difference (RCF versus LIME) with air mass for the different Cimel spectral bands. Percentiles 99 and 1 are included as horizontal lines.

Figures 5 and 6 represent the AOD differences (RCF versus RIMO/LIME) with the air mass. We observed maximum (percentile 99) differences (air mass equals to 1) of 0.12 in the case of RCF-RIMO and 0.06 in the case of RCF-LIME comparisons (0.095 in the case of the 1640 nm spectral band). The AOD difference has a strong dependence on the atmospheric air mass in both cases, confirming the presence of a calibration error as the most significant contribution to these discrepancies. Considering the low expected contribution of errors associated with AOD and solar Langley calculations, solar extraterrestrial irradiance, and the Gain calibration method, most of these differences are expected to be directly related to uncertainties in the E_0^M term. Therefore, these differences can serve as an estimation of E_0^M uncertainties, set at 0.06 (6%) in the case of LIME (coverage factor, k=3), and 2% for k=1. This estimation is higher (9% for k=3 and 3% for k=1) in the case of 1640 nm spectral band.

Another method to compare the LIME in comparison to RCF/RIMO in terms of lunar irradiances is presented in Figures 7 and 8. From the Beer-Lambert Law, we can directly compare ΔAOD·ma following the equation:

$$\frac{E_{0,model}^{M}}{E_{0,RCF}^{M}} = \exp\left(\Delta AOD \cdot m_a\right)$$

It can be seen ratios up to 6.3% in the case of the comparison RCF versus LIME, with more significant differences (up to 19.5%) in the case of RCF versus RIMO.

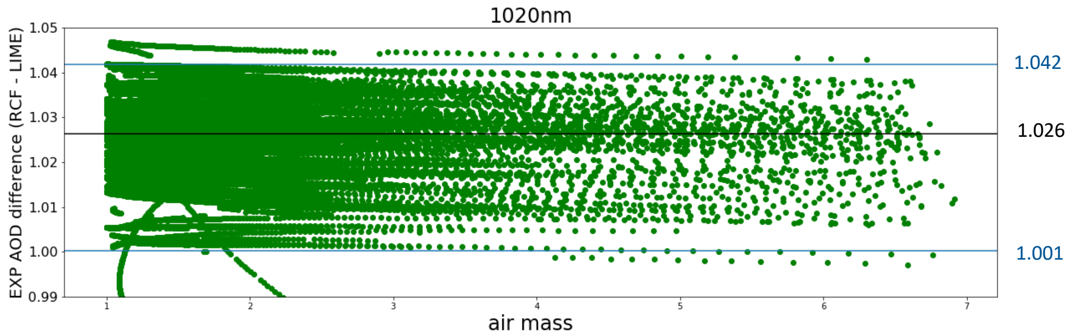
1020nm
EXP AOD difference (RCF - LIME)
air mass
1.042
1.026
1.001

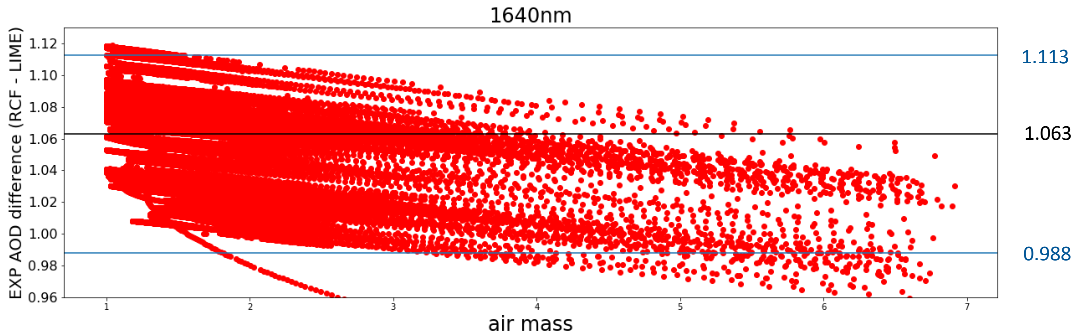
1640nm
EXP AOD difference (RCF - LIME)
air mass
1.113
1.063
0.988

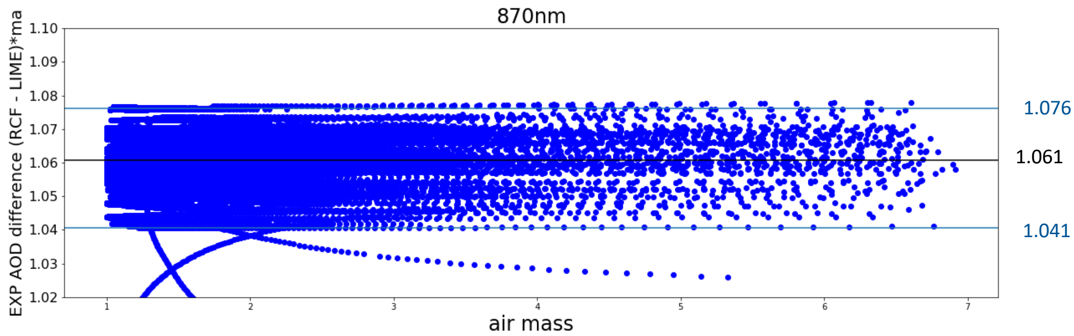
870nm
EXP AOD difference (RCF - LIME)*ma
air mass
1.076
1.061
1.041

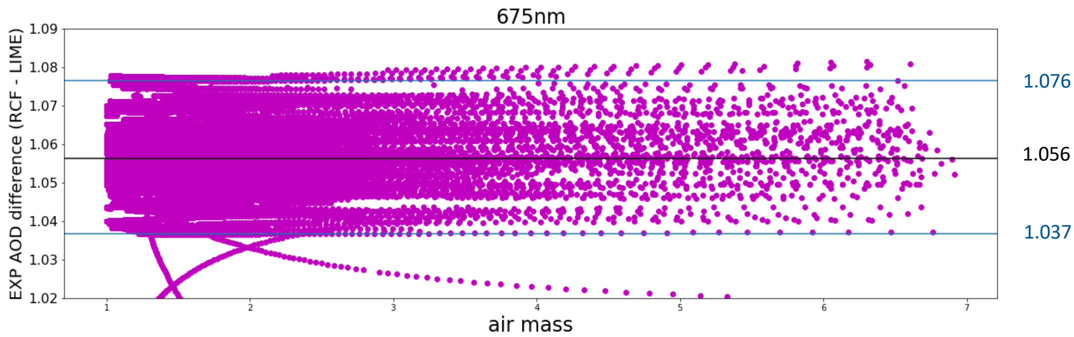
675nm
EXP AOD difference (RCF - LIME)
air mass
1.076
1.056
1.037

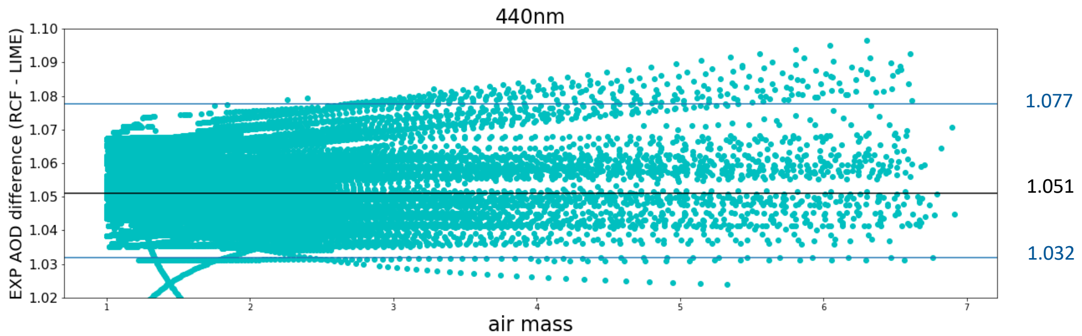
440nm
EXP AOD difference (RCF - LIME)
air mass
1.077
1.051
1.032

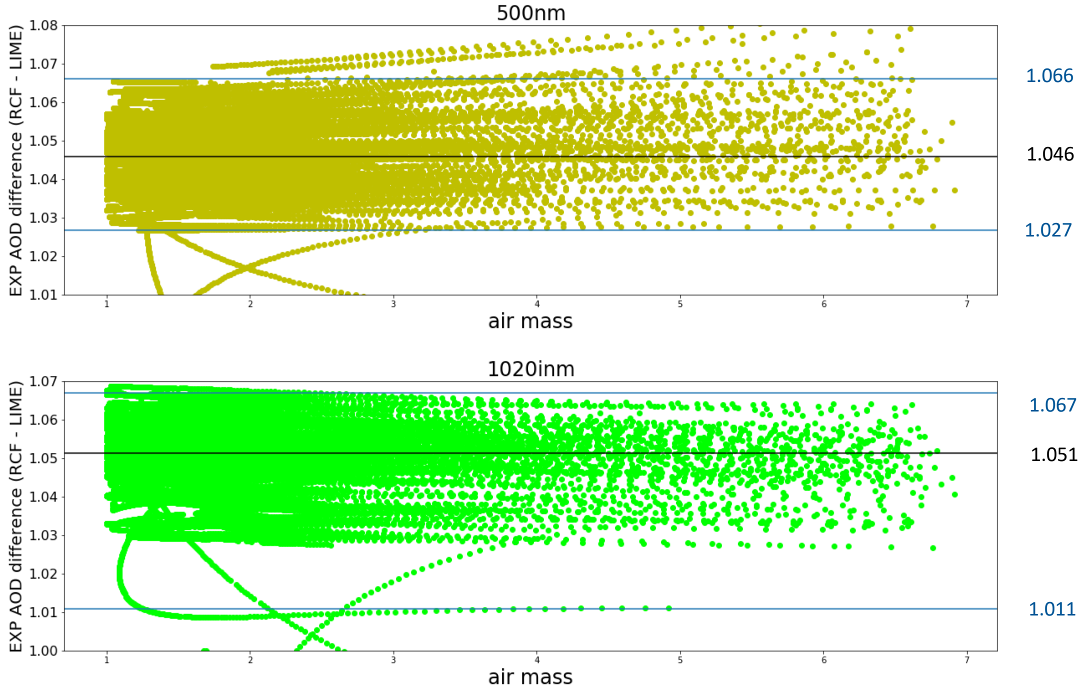

Figure 7: Exponential of AOD difference (RCF versus LIME) *ma against ma for the different Cimel spectral bands. Percentiles 99 and 1 are included as horizontal blue lines. Black line is the median.

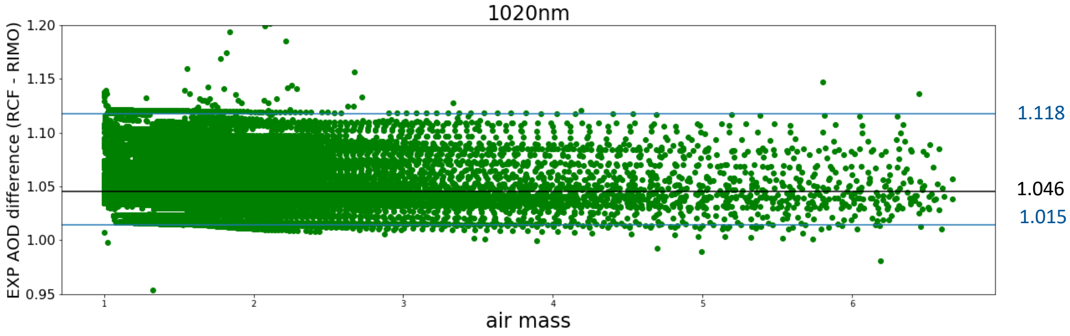
1020nm
EXP AOD difference (RCF - RIMO)
air mass
1.118
1.046
1.015

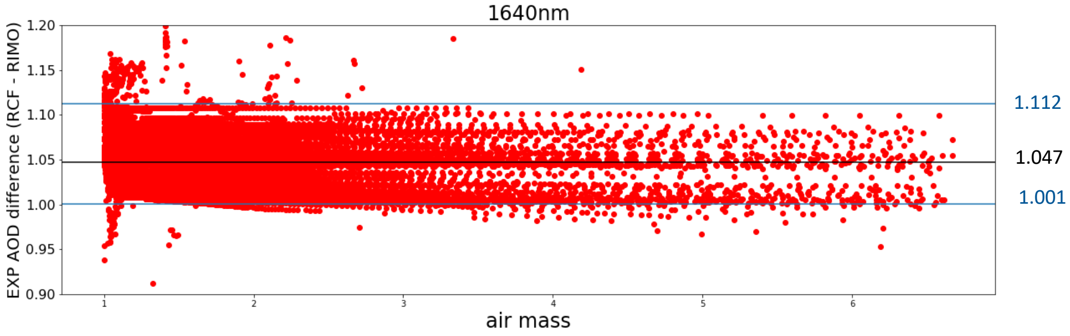
1640nm
EXP AOD difference (RCF - RIMO)
air mass
1.112
1.047
1.001

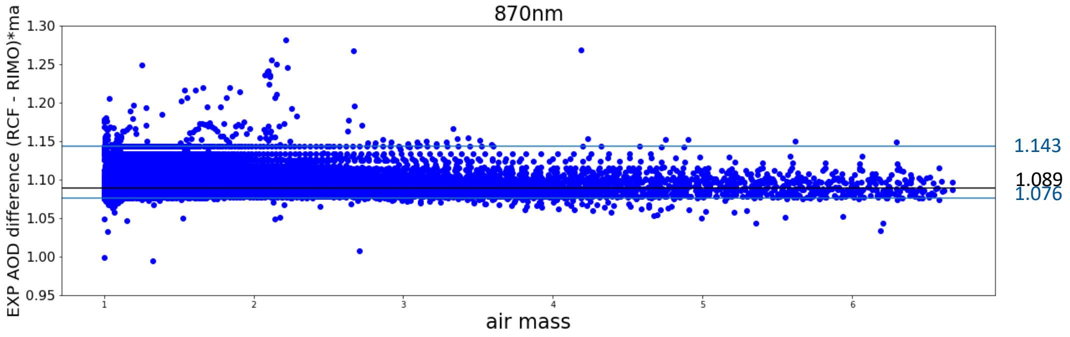
870nm
EXP AOD difference (RCF - RIMO)*ma
air mass
1.143
1.089
1.076

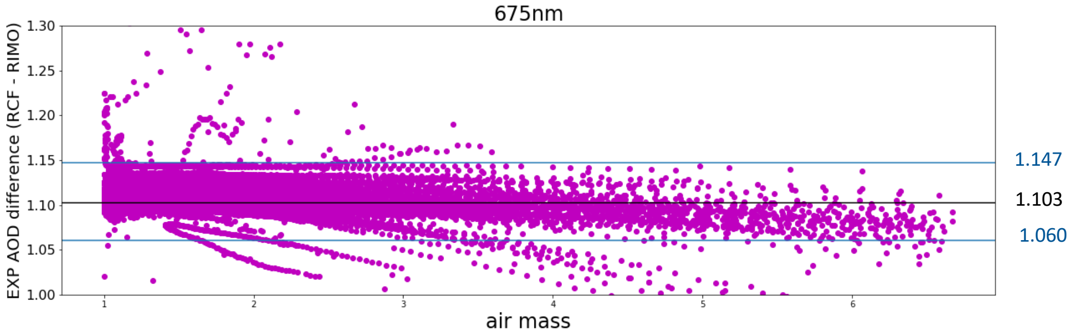
675nm
EXP AOD difference (RCF - RIMO)
air mass
1.147
1.103
1.060

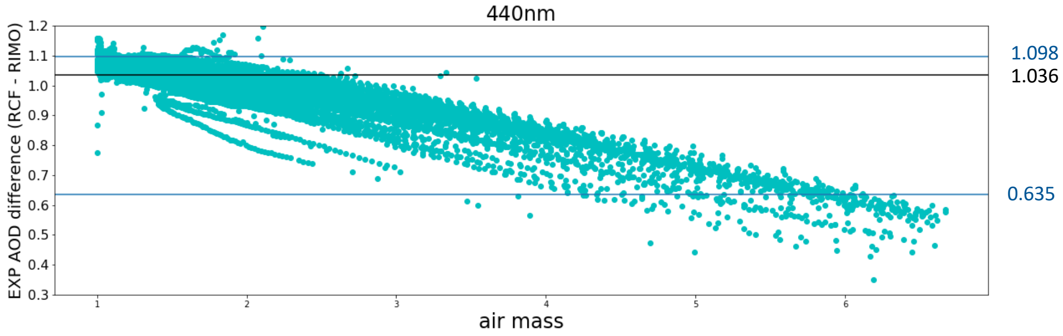
440nm
EXP AOD difference (RCF - RIMO)
air mass
1.098
1.036
0.635

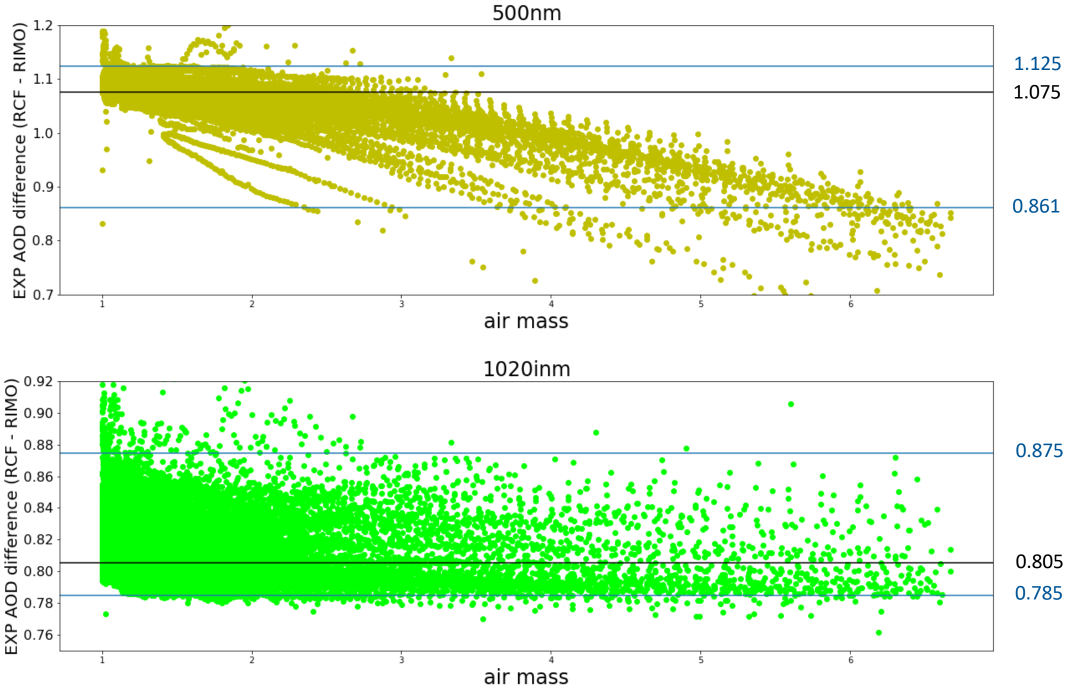

Figure 8: Exponential of AOD difference (RCF versus RIMO) *ma against ma for the different Cimel spectral bands. Percentiles 99 and 1 are included as horizontal blue lines. Black line is the median.

5 Conclusions

We can conclude from this report that the use of the LIME model introduces a substantial improvement in the calculation of AOD at night in comparison to the use of the ROLO/RIMO model. Our results show AOD departures from our references (the AOD retrieved using the RCF model) quite consistent to the 2% uncertainty limit expected for the LIME model. In this sense, standard errors below 0.014 have been found in the linear fitting analysis between AOD RCF and AOD LIME. The only exception was found for those Cimel spectral bands measuring with the InGaAs detector (1020i and 1640 nm), where a higher standard error was retrieved using LIME. In the case of 1640 nm we observed standard errors of 0.027 in the RCF versus LIME comparison in contrast to the value of 0.023 found in the comparison RCF versus RIMO. These differences are one order of magnitude higher in the case of RCF-LIME comparison at Silicon 1020 nm (0.001) with respect to InGaAs 1020 nm (0.016) spectral band. Similar conclusions can be extract from the analysis of AOD differences with the optical air mass.

However, despite of these good results, we have to admit that appreciable problems still exist in the LIME v01 irradiance model, associated to low phase angles (still needed more measurements near full moon), associated to the InGaAs spectral bands, but also to the rest of spectral bands in the view of the important zenith angle dependence of the AOD retrieved at night with the LIME model (Figures A2 and 6). On the other hand, the RCF was specifically designed to achieve accurate AOD, but not accurate extraterrestrial lunar irradiance in SI units. There are fundamental differences between LIME and RCF, the main one being the SI irradiance calibration of the measurements used to derive the LIME model. This is not existing in RCF, thus the RCF cannot be used to infer lunar irradiance, only AOD. However, the AOD retrieval with LIME is a good indication of the model uncertainty and helps monitoring the model performance.

D-5: Report on the impact of using the LIME model on the stability and accuracy of aerosol retrieval (day vs. night)

6 References

Barreto, A., Román, R., Cuevas, E., Pérez-Ramírez, D., Berjón, A., Kouremeti, N., Kazadzis, S., Gröbner, J., Mazzola, M., Toledano, C., Benavent-Oltra, J., Doppler, L., Juryšek, J., Almansa, A., Victori, S., Maupin, F., Guirado-Fuentes, C., González, R., Vitale, V., . . . Yela, M.: Evaluation of night-time aerosols measurements and lunar irradiance models in the frame of the first multi-instrument nocturnal intercomparison campaign. Atmospheric Environment, 202, 190-211. https://doi.org/10.1016/j.atmosenv.2019.01.006, 2019.

Berkoff, T. A., Sorokin, M., Stone, T., Eck, T. F., Hoff, R., Welton, E., and Holben, B.: Nocturnal aerosol optical depth measurements with a small-aperture automated photometer using the moon as a light source, J. Atmos. Ocean. Tech., 28, 1297–1306, doi:10.1175/JTECH-D-10-05036.1, 2011.

Giles, D. M., Sinyuk, A., Sorokin, M. G., Schafer, J. S., Smirnov, A., Slutsker, I., Eck, T. F., Holben, B. N., Lewis, J. R., Campbell, J. R., Welton, E. J., Korkin, S. V., and Lyapustin, A. I.: Advancements in the Aerosol Robotic Network (AERONET) Version 3 database – automated near-real-time quality control algorithm with improved cloud screening for Sun photometer aerosol optical depth (AOD) measurements, Atmos. Meas. Tech., 12, 169–209, https://doi.org/10.5194/amt-12-169-2019, 2019.

Herber, A., Thomason, L. W., Gernandt, H., Leiterer, U., Nagel, D., Schulz, K.-H., Kaptur, J., Albrecht, T., and Notholt, J.: Continuous day and night aerosol optical depth observations in the Arctic between 1991 and 1999, J. Geophys. Res.-Atmos., 107, AAC6.1–AAC6.13, doi:10.1029/2001JD000536, 2002.

Holben, B. N., Eck, T. F., Slutsker, I., Tanré, D., Buis, J. P., Setzer, A., Vermote, E., Reagan, J. A., Kaufman, Y. J., Nakajima, T., Lavenu, F., Jankowiak, I., and Smirnov A.: AERONET – A federated instrument network and data archive for aerosol characterization, Remote Sens. Environ., 66, 1–16, 1998.

Kieffer, H. H. and Stone, T. C.: The spectral irradiance of the moon, Astron. J., 129, 2887–2901, 2005.

Lacherade, S., Viticchié, B., Stone, T., Lebégue, L., Wagner, S., and Hewison, T.: On the phase-angle dependence of the moon calibration results, GSICS Quat: Lunar calibration, 7, 6–7, 2013.

Lacherade, S., Aznay, O., Fougnie, B., and Lebégue, L.: POLO: a unique dataset to derive the phase angle dependence of the Moon irradiance, Proc. SPIE 9241, Sensors, Systems, and Next-Generation Satellites XVIII, 924112 (7 October 2014), https://doi.org/10.1117/12.2067283, 2014.

Li, Z., Li, K., Li, D., Yang, J., Xu, H., Goloub, P., and Victori, S.: Simple transfer calibration method for a Cimel Sun–Moon photometer: calculating lunar calibration coefficients from Sun calibration constants, Appl. Optics, 55, 7624–7630, https://doi.org/10.1364/AO.55.007624, 2016.

Stone, T.C.; Kieffer, H.; Lukashin, C.; Turpie, K. The Moon as a Climate-Quality Radiometric Calibration Reference. Remote Sens., 12, 1837. https://doi.org/10.3390/rs12111837, 2020.

Viticchié, B., Wagner, S., Hewison, T., and Stone, T.: Lunar calibration of MSG/SEVIRI solar bands, GSICS Quat: Lunar calibration, 7, 3–5, 2013.

Wehrli, C.: Spectral Solar Irradiance Data (WMO ITD 149; Geneva: WMO), 1986.

A Appendix

A.1 Mean AOD differences

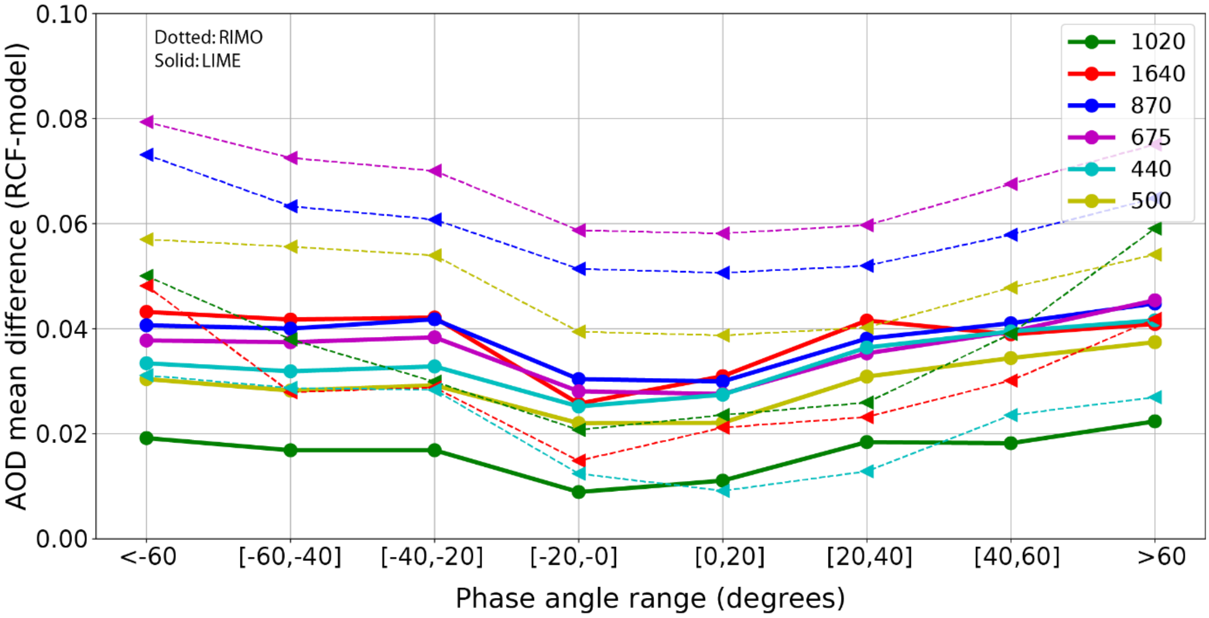

Figure A1: Mean AOD differences for different lunar phase angle ranges and CE318-TS spectral bands considering the AOD retrieved with the RCF as reference. Dotted lines indicate the difference with the AOD retrieved using RIMO and solid line is the same but using LIME as lunar exo-atmospheric irradiance model.

A.2 Zenith angle dependence

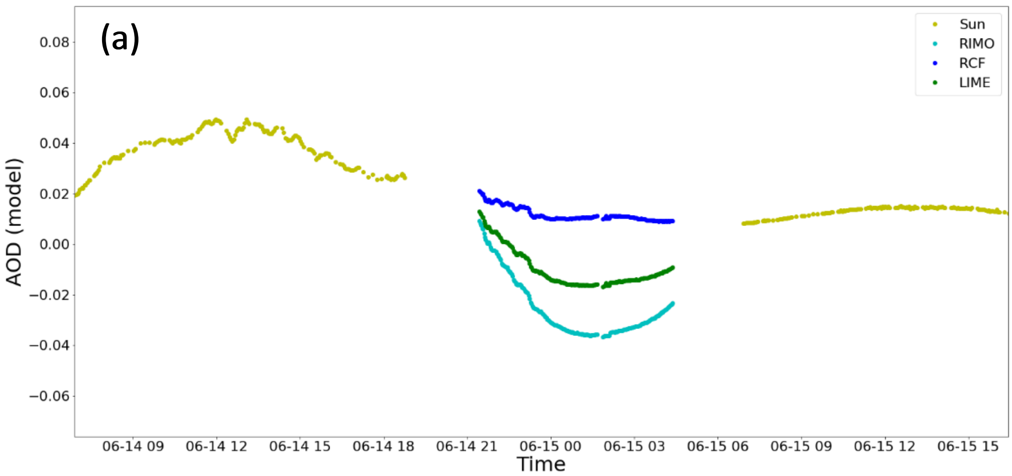

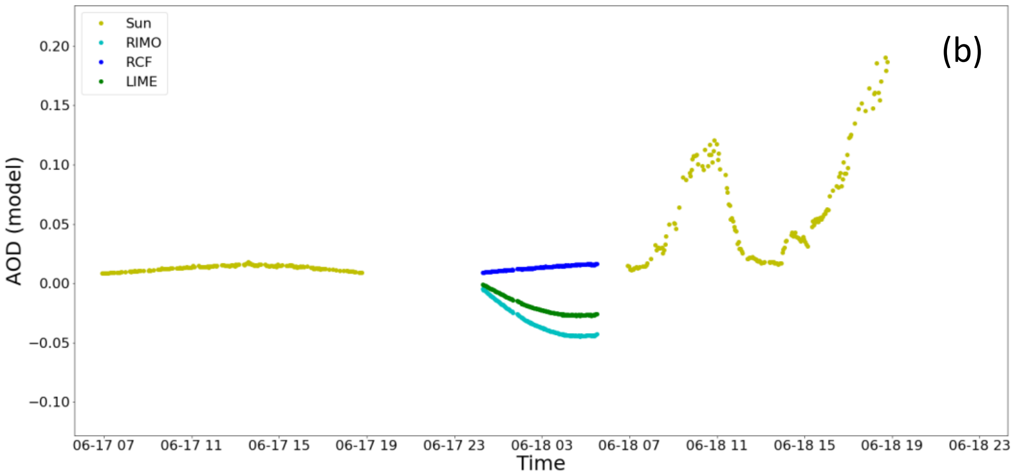

Figure A2: AOD measured at 870 nm at Teide Peak station for a sequence of two days (yellow) and one night at two lunar phase angles regimes (a) 15-16 June, 2022, near full moon, and (b) 17-18 June, 2022, near last quarter. Nocturnal AOD products were retrieved using RIMO, RCF and LIME as lunar extraterrestrial irradiance models.